Optical Materials 33 (2011) 413–418

Contents lists available at ScienceDirect

Optical Materials

journal homepage: www.elsevier.com/locate/optmat

Optical properties and gamma-ray response of Czochralski grown Pr:$Lu_3Al_5O_{12}$ scintillating garnet crystals with different Pr content

Takayuki Yanagida [a,*], Mitsuhiro Sato [a], Kei Kamada [a,b], Yutaka Fujimoto [a], Yuui Yokota [a], Akira Yoshikawa [a,c], Valery Chani [a]

[a] Institute of Multidisciplinary Research for Advanced Materials, Tohoku University, Sendai, Miyagi 980-8577, Japan
[b] Materials Research Laboratory of Furukawa Co. Ltd., 1-25-13 Kannondai, Tsukuba, Ibaraki, Japan
[c] New Industry Creation Hatchery Center (NICHe), Tohoku University, 6-6-10 Aoba, Aramaki, Aoba-ku, Sendai 980-8579, Japan

ARTICLE INFO

Article history:
Received 18 May 2010
Received in revised form 23 August 2010
Accepted 28 September 2010
Available online 20 October 2010

Keywords:
Scintillation detector
Single crystal
Energy resolution
Scintillation yield
Pr^{3+}-doped garnet

ABSTRACT

Pr:LuAG single crystalline scintillators with different Pr^{3+} concentration, 0.1, 0.18, and 0.22 mol% were grown by the Czochralski method. The crystals were cut to dimensions of $2.2 \times 2.2 \times 15$ mm^3 and polished, simulating sensors for Positron Emission Tomography (PET). Their absorption coefficients were examined, and the absorption strength was found to be proportional to the Pr concentration. The α-ray induced emission spectra of the samples demonstrated two emission lines peaking at 310 and 370 nm. The emission intensities in the radio luminescence spectra were also proportional to the Pr content. The absolute light yields and intrinsic energy resolution under γ-ray irradiation were evaluated at +20, 0, and −20 °C using avalanche photodiode as a photodetector. Pr 0.22% doped crystal had strongest light output of 16 400 ph/MeV, and its intrinsic energy resolution was around few % at several hundred keV. When coupled with PMT, the decay time was around 25 ns, and it was almost independent on concentration.

1. Introduction

Crystalline scintillators coupled with photo-detectors have been used in many fields, such as high energy particle physics, astrophysics, medical imaging, security, and resource exploration. For every application, the crystals with certain combination of physical properties are desired. For example, medical imaging requires high stopping power, high light yield, and fast decay. Up to now, Ce^{3+}-doped materials have been well studied to obtain a very fast and efficient emission centers. The emission around 350–550 nm is mostly observed when oxide host crystals are doped with Ce^{3+}. Therefore, Ce^{3+} is widely used as a dopant. For example, Ce:Gd_2SiO_5 (Ce:GSO) [1], Ce:Lu_2SiO_5 (Ce:LSO) [2], and Ce:$(Lu,Y)_2SiO_5$ (Ce:LYSO) [3] crystals are well known and efficient materials for radiation measurements.

Development of Pr:$Lu_3Al_5O_{12}$ garnet (hereafter Pr:LuAG) was recently reported [4–6]. The density of LuAG is about 6.73 g/cm^3, and its effective atomic number is 63. It is known that in the wide band-gap materials with medium or high crystal field strength, the Pr^{3+} ion demonstrates 5d–4f emission due to the dipole transition. Pr^{3+} is supposed to be a candidate for a competitive emission center in the scintillating materials with high figure of merit. That is why, number of studies on Pr:$Y_3Al_5O_{12}$ (Pr:YAG) [7], $YAlO_3$ (Pr:YAP) [8,9], and Pr:LSO [10], have been done in the past. When LuAG garnet is doped with Pr^{3+}, this scintillator demonstrates high stopping power due to Lu, fast decay, and high light yield that is three times greater than that of $Bi_4Ge_3O_{12}$ (BGO) [5]. When the physical shape of the crystal is cuboids or thin plate, the potential energy resolution of the Czochralski (Cz) grown Pr:LuAG exhibits 4–5% at several hundred keV [11,12]. Additionally, in order to decrease an emission from a host, Ga-substituted Pr:$Lu_3(Ga_xAl_{1-x})_5O_{12}$ crystals were also studied [13,14].

Recently, Pr:LuAG was considered as a detector material for Positron Emission Mammography [15]. For such application, 4 in. diameter Pr:LuAG crystals were grown by the Cz method, and thus, successful industrial scale production of Pr:LuAG was demonstrated. However, there is still a room for detailed research, because only few tests have been done to understand the relation between Pr concentrations and scintillation properties of the Cz grown Pr:LuAG crystals. As an example, Pr:LuAG crystals which had different Pr concentration were grown by the micro-pulling down method [16] and evaluated.

It was also reported that the light yield decreased [17] when Pr concentration increased from 1.5 to 10 mol% considering nominal values (melt composition). However, actual content of Pr in the

* Corresponding author. Address: Institute of Multidisciplinary Research for Advanced Materials, Tohoku University, 2-1-1 Katahira, Aoba-ku, Sendai 980-0812, Japan. Tel.: +81 22 217 5822; fax: +81 22 217 5102.
E-mail address: t_yanagi@tagen.tohoku.ac.jp (T. Yanagida).

0925-3467/$ - see front matter © 2010 Elsevier B.V. All rights reserved.
doi:10.1016/j.optmat.2010.09.023

grown crystals is fundamentally different from Pr content in the melt because of segregation. Thus, the melt containing 10% of dopant does not always produce 10%-doped crystal. Moreover, there is a limit of solubility in the solid state that depends on crystallographic structure of the host crystal and nature of the dopant. When the dopant concentration in the crystal exceeds the solubility limit, the second phase formation is observed. As a result, the crystal loses its transparency particularly due to formation of interfaces between the host crystal and secondary phase inclusions. Thus, it is evident that "nominal" concentration of the dopant in the melt is generally meaningless. Instead, actual dopant concentration in the solid crystal should be considered to understand dependence of optical properties on dopant content. To examine actual dopant concentration, the Electron Probe Micro Analyzer (EPMA) or other quantitative instruments such as Inductively Coupled Plasma Mass Spectrometry (ICP-MS), Secondary ion mass spectrometry (SIMS), and others should be used depending on the concentration of the dopant.

In the present communication, we report on evaluation of scintillation responses of the Czochralski grown Pr:LuAG crystals produced with different Pr concentrations. The specimens of rectangular shape with dimensions of $2.2 \times 2.2 \times 15\ mm^3$ were systematically tested assuming their possible application in Positron Emission Mammography (PEM). As it was mentioned above, production of Pr:LuAG crystals approximates industrial phase. Therefore, their evaluation assuming actual application is required. The reason of application of Si-APD (avalanche photodiode) as a photodetector was based on our intention to develop Pr:LuAG and pixilated APD based gamma-camera for PET-MRI application in national project [18]. Fig. 1 illustrates the APD used in the present work and the Pr:LuAG crystals. The decay time measurements were performed with a photomultiplier tube (PMT). The actual Pr concentrations in the crystals were examined by EPMA, and the as measured actual concentrations of Pr were 0.1, 0.18, and 0.22 mol% [19].

2. Experimental procedures

2.1. Optical properties

In order to grasp optical properties of the LuAG specimens, the absorption coefficient and emission spectra were measured. The transmittance was evaluated by JASCO V-550 spectrofluorometer. After corrections for the reflections by Shimadzu UV-2550 spectrofluorometer and determination of the samples thickness, the absorption coefficients were determined. The calculations were performed according to the Lambert–Beer law. Then, the emission spectra were examined by the Edinburgh F920 spectrometer under

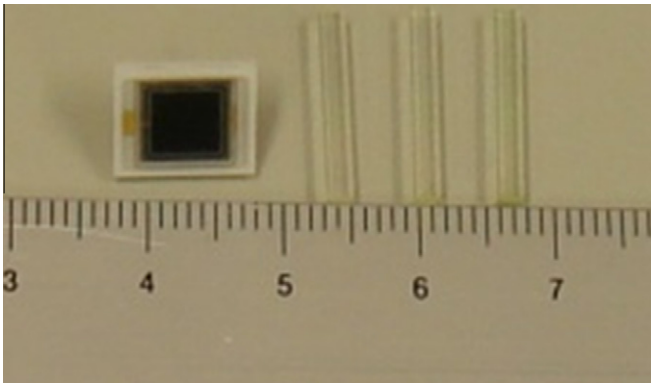

Fig. 1. From left to right, APD S8664–55, Pr 0.10 mol%, 0.18 mol%, and 0.22 mol% doped LuAG crystals.

^{241}Am α-ray excitation, imitating the radiation measurement. All the optical properties were measured from specimens with wide surface area ($2.2 \times 15\ mm^2$) following design of our instruments.

2.2. γ-ray induced scintillation properties

Based on the emission spectra described later, Pr:LuAG crystals emit with fluorescence peaks centered at wavelength of 310 and 370 nm. Therefore, the reflectors such as Enhanced Specular Reflector (ESR) film or Teflon, which are generally used reflectors to correct photons in visible wavelength range, were not suitable for this type of scintillator. To gather such ultra violet (UV) photons, $BaSO_4$ reflector was used. The $BaSO_4$ was firstly dissolved in water, and then painted onto the scintillating samples. After drying-out, the samples were coated with $BaSO_4$ layer that demonstrated considerable improvement in photon collection efficiency of Pr:LuAG.

As a photo-detector, APD S8664-55 (Hamamatsu) with $5 \times 5\ mm^2$ light window was used. This device has higher quantum efficiency (QE) than normal PMT in the emission wavelength of Pr:LuAG (from 310 to 370 nm). The typical QE was 40%.

The APD (Hamamatsu, S8664-55) was optically coupled with the sample scintillators with silicone grease (OKEN, 6262A) that was placed between corresponding surfaces. The size of the light sensitive window of the APD was 5×5 and $2.2 \times 2.2\ mm^2$ square surfaces of the Pr:LuAG samples was attached to the APD imitating PET arrangement. Once the radiation was detected by the scintillator, the signals from the APD were fed into a pre-amplifier (CP580K), a shaping amplifier (CP 4417) with 2 μs shaping time, a pocket MCA (Amptec 8000A), and finally to a PC. The bias voltage for the APD (about 300 V) was supplied by CP 6641 power source. As for the decay time measurements, the PMT (Hamamatsu R6231) was used as a light detector instead of the APD, because a raw signal originated from APD was weak. In this setup, the light yield and its non-proportionality were studied in the energy range from 59.5 to 1408 keV using irradiation produced from ^{241}Am, ^{22}Na, ^{137}Cs, ^{133}Ba, and ^{152}Eu sources at each temperature. Through all the experiments related to the γ-ray responses, the measurements were performed at three different temperatures (+20, 0, and −20 °C). The temperature of the specimens was controlled by a heat bath with accuracy of ±0.5 °C. Thus, the temperature dependences were analyzed. It is noted that in some applications, improvement of the signal-to-noise ratio is achieved through decreasing temperature of the detectors.

2.3. Procedures to determine intrinsic resolution

In order to evaluate the intrinsic energy resolution, the basic properties of the APD should be examined in advance. Intrinsic energy resolution is expressed as follows:

$$\Delta E^2 = \delta_{int}^2 + \delta_{stat}^2 + \delta_{noize}^2 \quad (1)$$

where ΔE represents the observed energy resolution, δ_{int} is the intrinsic energy resolution of the scintillator, δ_{stat} is statistical contribution, and δ_{noize} is the APD noise contribution. The second term in the right hand side of equality (1) is represented as

$$\delta_{stat} = 2.36(F/N_{e-h})^{0.5} \quad (2)$$

where F stays for the excess noise factor, and N_{e-h} is the number of electron–hole pairs. The excess noise factor is the fluctuation of the avalanche gain M as $F = \langle M^2 \rangle / \langle M \rangle^2$. The last term is a contribution from the noise expressed as

$$\delta_{noize} = (\Delta_{noise}/N_{e-h}) = 2.36\sigma_{noise}/N_{e-h} \quad (3)$$

In this formula, Δ_{noise} means the normalized noise component and Δ_{noise} represents the dark noise expressed in rms electrons.

In order to determine these values, the avalanche gain M, which is the function of supplied bias voltage, temperature, and light wavelength, must be measured. The M value was determined by illumination of UV LED (~365 nm emission), which simulates fluorescence from Pr:LuAG, and the photocurrent of the APD was recorded using the Keithley 237 High-Voltage Source-Measure Unit. The LED was operated in DC mode and the photocurrent at V = 0 was approximately 100 times as high as the dark current. Fig. 2 illustrates the results of these measurements performed at three different temperatures of 20, 0, and −20 °C. The multiplication gain M below the voltage of about 100 V remained close to unity because multiplication region was still not formed. When the voltage exceeded 100 V, the bias dependence of the multiplication became observable. Moreover, the gain M increased with APD cooling because the mean free path for phonon scattering became shorter.

Considering the detection of scintillation lights or light pulse, F can be interpreted as the gain non-uniformity, which contributes to the peak broadening, $F^{1/2}$ times as wide as the peak width, which is estimated from the Poisson distribution of the primary e–h pairs generated. Thus, FWHM of the peak for light pulses, Δ_{LED}, is described as

$$\Delta^2_{LED} = 2.35^2 \times F/N_{e-h} + \Delta^2_{noise} \quad (4)$$

where Δ_{noise} is FWHM of the peak contributed from the circuit noise [20,21].

At first, in order to evaluate circuit noise Δ_{noise}, a test pulse was injected into the pre-amplifier, and the width of the test pulse peak, ΔP_{noise}, was recorded. Then, under the same experimental conditions, the UV LED was used as a source of the light pulse to measure the pulse height, P, and its width, ΔP_{LED}. Here, Eq. (4) is described as

$$(\Delta P_{LED}/P)^2 = F/N_{e-h} + (\Delta P_{noise}/P)^2 \quad (5)$$

Finally, we irradiated 5.9 keV X-ray which generated 1640 electron–hole pairs to determine the number of the primary e–h pairs, N_{e-h} in the pulse height spectra obtained in the previous experiments. Fig. 3 presents an example of the pulse height spectra. However, in order to evaluate N_{e-h} of P, the discrepancy of the gain M for the X-rays and the light signals should be taken into account. As a result, F value for the APD used in our experiments was estimated to be ~2 in normal operation range ($10 < M < 100$).

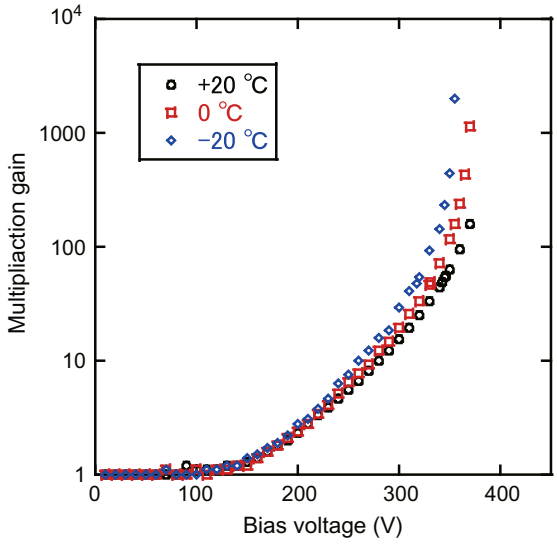

Fig. 2. The avalanche gain plotted against the bias voltage.

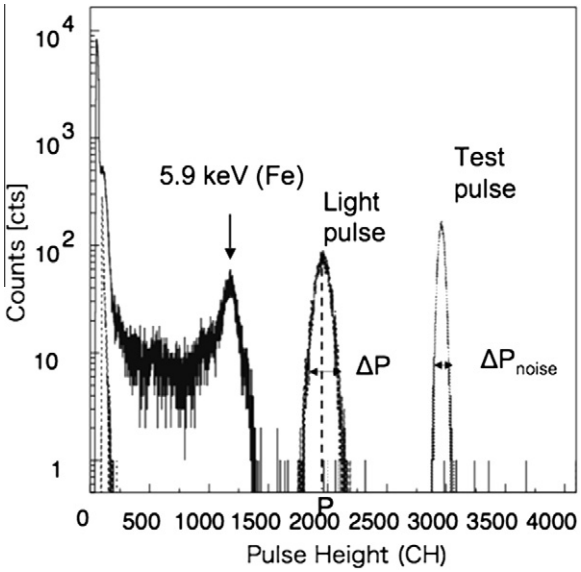

Fig. 3. The energy spectra of 5.9 keV X-ray, light and test pulse generator peaks at the gain $M = 10$, −20 °C.

3. Results and discussion

3.1. Optical properties

The absorption coefficient results are demonstrated in Fig. 4. Three peaks positioned around 200, 240, and 280 nm wavelengths were identified as those attributed to Pr^{3+} absorption. The absorption coefficients of the peaks centered at 240 and 280 nm lines were saturated at about 35 cm^{-1} because of the detection limit of the instrument used for the transmittance measurements. The 200 nm absorption was assigned to the perturbed exciton or Pr^{3+}-related charge-transfer states [22]. The absorption bands at 240 and 280 nm were ascribed to the two lowest $4f(^3H_4) \rightarrow 5d_{2,1}$ transitions of Pr^{3+}. 4f–4f absorption peaks around 500 nm (^3P_x, $x = 0, 1, 2 \rightarrow {}^3H_4$) and 600 nm ($^1D_2 \rightarrow {}^3H_4$) were considerably weaker when compared with those of the 5d–4f absorption lines. At 220 and 260 nm where no saturation was observed, the absorption coefficients were proportional to Pr concentrations, and this result is consistent with EPMA analysis for the actual Pr concentrations.

Fig. 5 represents the emission spectra of the crystals excited by 5.5 MeV α-ray radiation supplied from ^{241}Am in order to imitate γ-ray based applications. In this case, the host lattice was excited instead of emission centers. At these spectra, the emission peaks have been detected at 310 and 370 nm for all the samples. These peaks were similar to those obtained under excitation with UV photons [12,13], and both lines were originated from the transitions from lowest 5d state to ^3H_x 4f states.

3.2. Scintillation responses

The light yield (LY) of these Pr:LuAG samples was calibrated from ^{55}Fe direct irradiation peak to APD. In view of the fact that the average number of electron–hole pairs created in the photoelectric event in silicon is known, the LY for each sample can be calculated. In 0.22% Pr-doped LuAG, about 6500 electron–hole pairs was generated per 1 MeV. Since the QE of APD is ~40% at 310 nm, LY of this sample becomes ~16 400 ph/MeV. This is about three times greater than that of the reference BGO scintillating crystal examined with same experimental setup (5300 ph/MeV, QE corrected). Fig. 6 illustrates an example of the pulse height spectrum of Pr 0.22% doped sample irradiated by ^{137}Cs, where

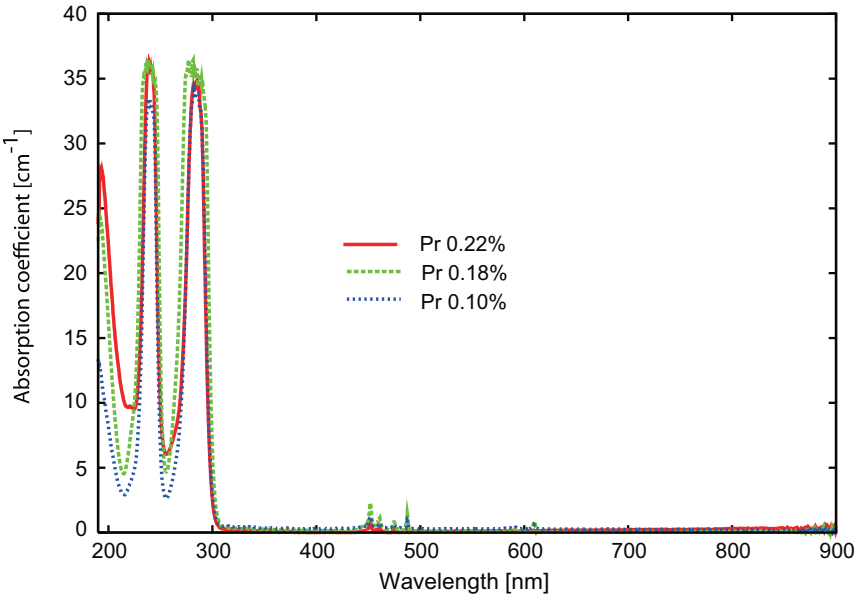

Fig. 4. Absorption coefficients of Pr:LuAG. Red, green, and blue represent 0.22 mol%, 0.18 mol%, and 0.10 mol% Pr-doped crystals, respectively. (For interpretation of the references to colour in this figure legend, the reader is referred to the web version of this article.)

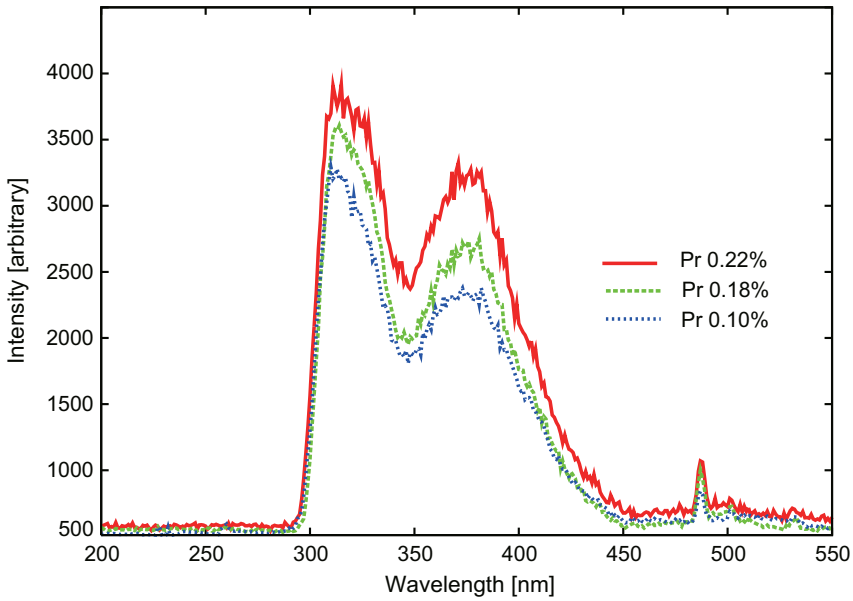

Fig. 5. ^{241}Am a-ray excited emission spectra of Pr:LuAG. Red, green, and blue represent 0.22 mol%, 0.18 mol%, and 0.10 mol% Pr-doped crystals, respectively. (For interpretation of the references to colour in this figure legend, the reader is referred to the web version of this article.)

the photo-absorption peak and the Compton edge are clearly observed. The relation between energy and pulse height was evaluated using 59.5 keV (Am), 511 keV (Na), 1274 keV (Na), 356 keV (Ba), 1408 keV (Eu), and 662 keV (Cs). As long as other photo-absorption peaks were observed, their pulse-height and energy relations were also involved in the evaluation. Fig. 7 shows a non-proportional relation at three different temperatures. In this measurement, we just put fitting errors in the figure. This result suggests that Pr:LuAG is applicable to not only the PET with monochromatic energy sources (511 keV), but also to the instruments that register irradiation of keV to MeV energy range.

Fig. 8 summarizes the light yield of Pr:LuAG samples that was observed at three temperatures. In view of the temperature dependence, the *LY* decreased monotonically when the temperature decreased. Similar phenomenon was observed in the Ce-doped YAG crystals, and it is probably initiated by the effect of acceleration detrapping from shallow traps [23]. Moreover, according to Fig. 8, the *LY* is proportional to Pr concentration in the garnet host matrix, and there is no sign of concentration quenching. Judging from this tendency, increasing of the Pr^{3+} in the host lattice would increase *LY*.

The intrinsic energy resolution is illustrated in Fig. 9. In this measurement, we consider both systematic and fitting errors. As a results, the intrinsic resolutions were few % at several hundreds keV and, and no temperature dependence was observed. These findings are consistent with previous studies that demonstrated excellent energy resolution of Pr:LuAG crystals when the samples had cubic or thin plate shapes [10,11]. The important point is that

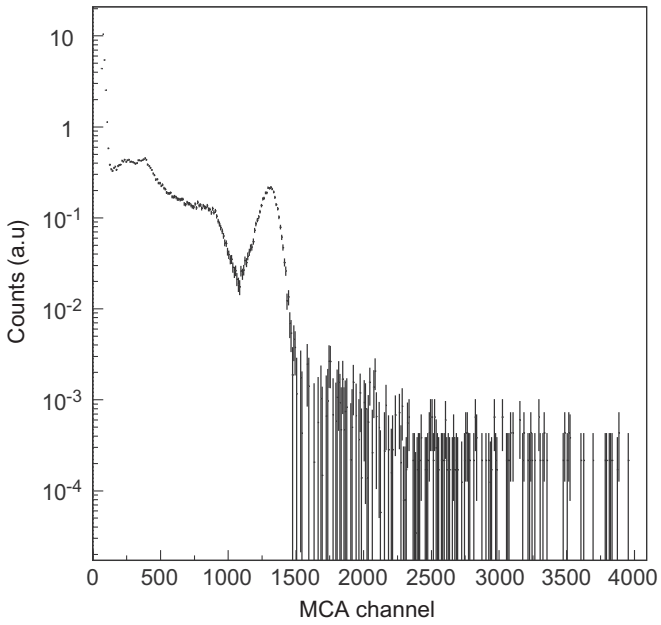

Fig. 6. ^{137}Cs pulse height spectrum of 0.22 mol% doped sample at 20 °C.

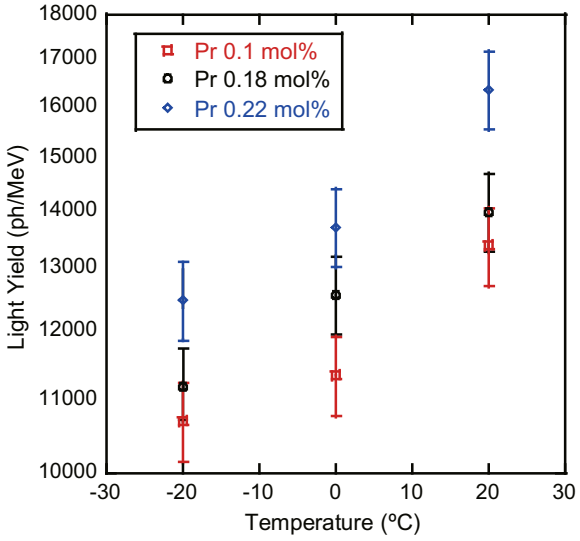

Fig. 7. From top to bottom, light yield non-proportionality of 0.22 mol%, 0.18 mol%, and 0.10 mol% Pr-doped LuAG, respectively. Black, red, and blue correspond to measurement temperatures of +20, 0, and −20 °C, respectively. (For interpretation of the references to colour in this figure legend, the reader is referred to the web version of this article.)

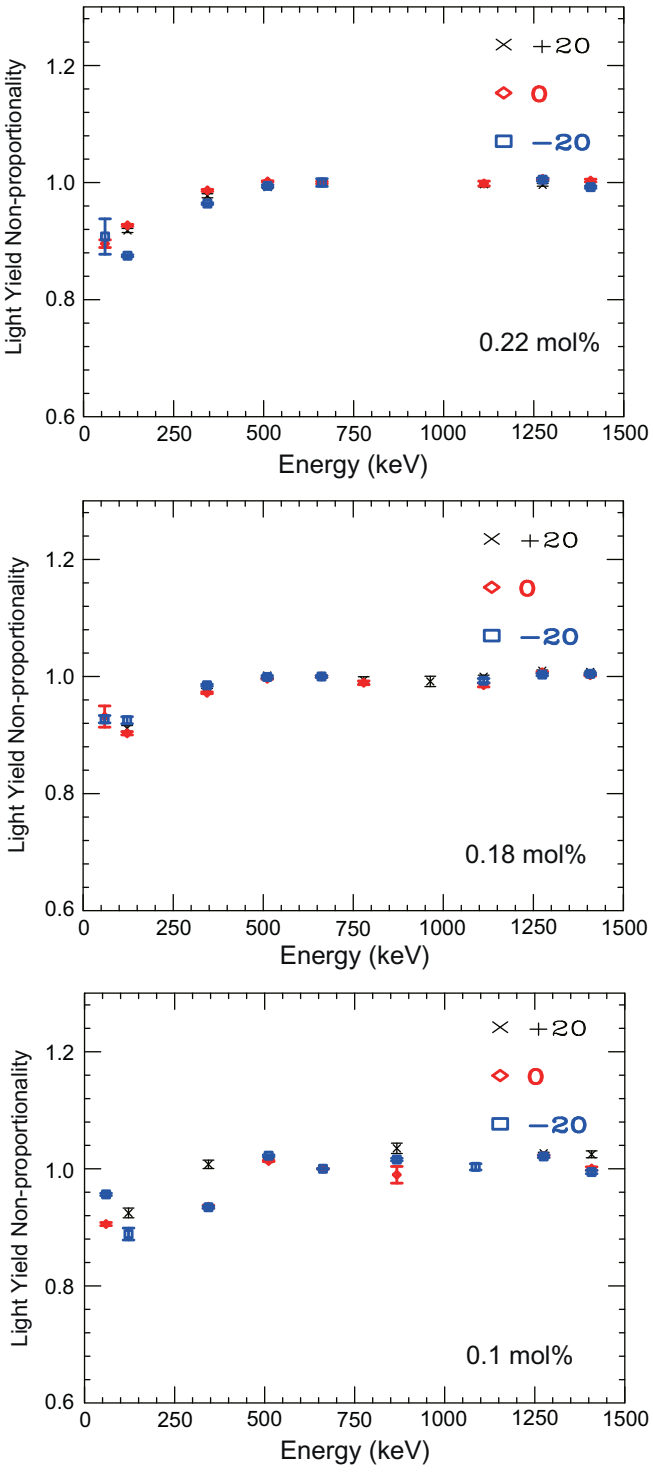

Fig. 8. The absolute light yield of the crystals with different Pr concentration plotted against the measurement temperature.

the crystalline samples discussed here had high aspect ratio assuming that their performance as prototypes for PET applications. If it is possible to reduce any noises and to select adequate avalanche gain, then high energy resolution could be expected in actual application of Pr:LuAG crystals. Similar to the light yield, 0.22% Pr-doped sample showed the best intrinsic energy resolution. Thus, within the Pr concentration range analyzed here, the optimal actual dopant concentration in the garnet phase was 0.22%.

Finally, Fig. 10 represents decay time constants as a function of the temperature. Within the error bars, no significant variations were observed in performance of the crystals containing different amount of Pr doping cations. As for temperature dependence, the general tendency was as follows: the scintillation decay time constants decreased (fast decay) when the specimens were heated. The observed values (25 ns) were slightly less than those observed previously (20–23 ns) possibly due to the difference in the crystalline quality of the specimens. Generally, the combination of the scintillation properties of Pr:LuAG crystals, including the *LY*, energy resolution, decay time constants, and operation performance at increased temperatures is close to that of ideal scintillating material.

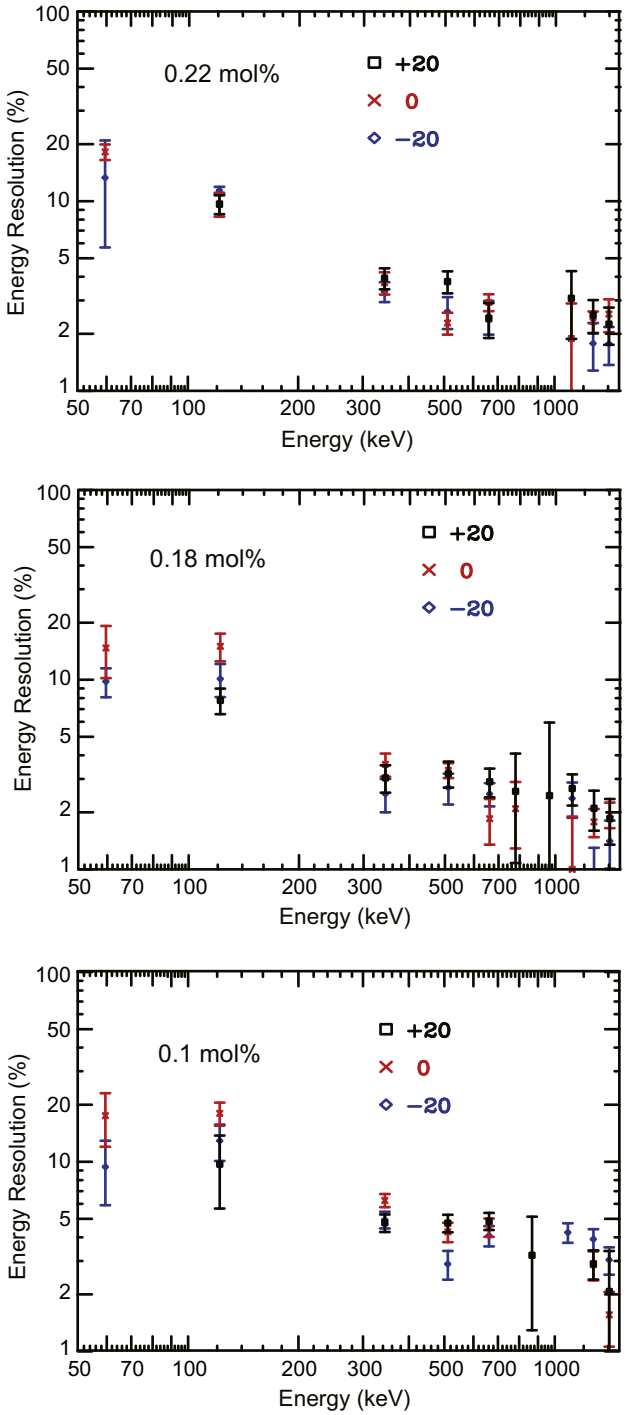

Fig. 9. Intrinsic energy resolution plotted against gamma-ray energy. Black, red, and blue represent measurement temperature of +20, 0, and −20 °C, respectively. (For interpretation of the references to colour in this figure legend, the reader is referred to the web version of this article.)

4. Summary

0.1, 0.18, and 0.22 mol% Pr^{3+}-doped $Lu_3Al_5O_{12}$ garnet crystals were grown by the Czochralski method. The crystals were cut to the specimens with dimension of $2.2 \times 2.2 \times 15\ mm^3$ for better simulating PET application. The absorption coefficients of the crystals were proportional to the actual Pr concentrations, and α-ray excited emission spectra were similar to those of γ-ray induced radio- or photo-luminescence spectra. The 0.22 mol% sample had highest light yield of 16 400 ph/MeV. The intrinsic resolution was few % at the level of several hundreds keV. The intrinsic energy resolution demonstrated dependence on Pr concentration, and it was practically independent on temperature. The main component of the decay time was around 25 ns for all the crystals.

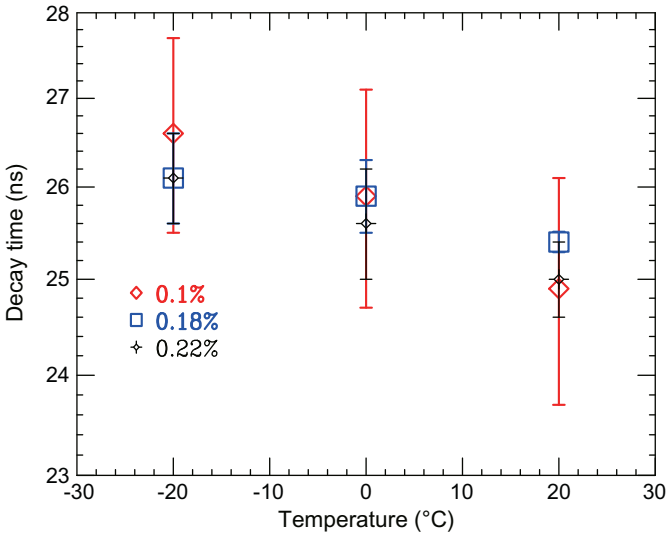

Fig. 10. Decay time constants of the crystals with different Pr concentrations plotted against the temperature.

References

[1] K. Takagi, T. Fukazawa, Appl. Phys. Lett. 42 (1983) 46.
[2] C.L. Melcher, J.S. Schweitzer, C.A. Peterson, Inorganic Scintillators and Their Application, Delft University Press, 1995.
[3] L. Qin, H. Li, S. Ding, G. Ren, J. Cryst. Growth 281 (2005) 518.
[4] H. Ogino, A. Yoshikawa, M. Nikl, A. Krasnikov, K. Kamada, T. Fukuda, J. Cryst. Growth 287 (2006) 335.
[5] H. Ogino, A. Yoshikawa, M. Nikl, K. Kamada, T. Fukuda, J. Cryst. Growth 292 (2006) 239–242.
[6] M. Nikl, H. Ogino, A. Krasnikov, A. Beitlerova, A. Yoshikawa, T. Fukuda, Phys. Status Solidi A 202 (2005) R4.
[7] W. Drozdowski, T. Lukasiewicz, A. Wojtowicz, D. Wisniewski, J. Kisielewski, J. Cryst. Growth 275 (2005) 709.
[8] C. Pedrini, D. Bouttet, C. Dujardin, B. Moine, J. Dafinei, P. Lecoq, M. Koseija, K. Blazek, Opt. Mater. 3 (1994) 81.
[9] C. Dujardin, C. Pedrini, J.C. Gâcon, A.G. Petrosyan, A.N. Belsky, A.N. Vasil'ev, J. Phys.: Cond. Matter 9 (1997) 5229.
[10] M. Nikl, H. Ogino, A. Yoshikawa, E. Mihokova, J. Pejchal, A. Beitlerova, A. Novoselov, T. Fukuda, Chem. Phys. Lett. 410 (2005) 218.
[11] L. Swiderski, M. Moszyński, A. Nassalski, A. Syntfeld-Kazuch, T. Szcz˛eśniak, K. Kamada, K. Tsutsumi, Y. Usuki, T. Yanagida, A. Yoshikawa, W. Chewpraditkul, M. Pomorski, IEEE Trans. Nucl. Sci. 56 (2009) 2499–2505.
[12] W. Drozdowski, P. Dorenbos, J.T.M. de Haas, R. Drozdowska, K. Kamada, K. Tsutsumi, Y. Usuki, T. Yanagida, A. Yoshikawa, IEEE Trans. Nucl. Sci. 55 (2008) 2420–2424.
[13] M. Nikl, J. Pejchal, E. Mihokova, J.A. Mares, H. Ogino, A. Yoshikawa, T. Fukuda, A. Vedda, C. D'Ambrosio, Appl. Phys. Lett. 88 (2006) 141913–141916.
[14] H. Ogino, A. Yoshikawa, M. Nikl, J. Pejchal, T. Fukuda, Jpn. J. Appl. Phys. 46 (2007) 3514–3517.
[15] T. Yanagida et al., IEEE Trans. Nucl. Sci. 57 (2010) 1492.
[16] A. Yoshikawa, M. Nikl, G. Boulon, T. Fukuda, Opt. Mater. 30 (2007) 6.
[17] W. Drozdowski, P. Dorenbos, R. Drozdowska, A.J.J. Bos, N.R.J. Poolton, M. Tonelli, M. Alshourbagy, IEEE Trans. Nucl. Sci. 56 (2009) 320–327.
[18] K. Kamada, T. Yanagida, J. Kataoka, A. Yoshikawa, A. Fukabori, K. Tsutsumi, T. Endo, Y. Usuki, In: IEEE NSS MIC 2009 Conference Record, 2009, pp. 1949–1951.
[19] K. Kamada, K. Tsutsumi, Y. Usuki, H. Ogino, T. Yanagida, A. Yoshikawa, IEEE Trans. Nucl. Sci. 55 (2008) 1488–1491.
[20] M. Moszynski, W. Czarnacki, W. Klamra, M. Szawlowski, P. Schotanus, M. Kapusta, Nucl. Instrum. Methods A 505 (2003) 63–67.
[21] M. Moszynski, M. Szawlowski, M. Kapusta, M. Balcerzyk, Nucl. Instrum. Methods A 485 (2002) 504.
[22] V. Babin, A. Krasnikov, Y. Maksimov, K. Nejezchleb, M. Nikl, T. Savikhina, S. Zazubovich, Opt. Mater. 30 (2007) 30.
[23] E. Zych, C. Brecher, J. Glodo, J. Phys.: Cond. Matter 12 (2000) 1947.